Elemental composition and mineralogical characteristics of volcanic ash and soil affected by the eruption of Mount Semeru, East Java

by Dwi Fitri Yudiantoro

Journal of Degraded and Mining Lands Management
Volume 11, Number 3 (April 2024):0000-0000, doi:10.15243/jdmlm.2024.113.0000
ISSN: 2339-076X (p); 2502-2458 (e), www.jdmlm.ub.ac.id

Research Article

Elemental composition and mineralogical characteristics of volcanic ash and soil affected by the eruption of Mount Semeru, East Java

Tri Candra Setiawati [1], Mohamad Nurcholis[2*], Basuki[1], Subhan Arif Budiman[1], Dwi Fitri Yudiantoro[3]

[1] Soil Science Department, Faculty of Agriculture, University of Jember, Jember 68121, Indonesia
[2] Soil Science Department, Faculty of Agriculture, Universitas Pembangunan Nasional Veteran Yogyakarta, Yogyakarta 55283, Indonesia
[3] Department of Geological Engineering, Faculty of Mineral Technology, Universitas Pembangunan Nasional Veteran Yogyakarta, Yogyakarta 55283, Indonesia

*corresponding author: nurcholis@upnyk.ac.id

Article history:
Received 14 October 2023
Revised 3 February 2024
Accepted ……………..

Keywords:
heavy metal elements
rare minerals
Tephra
volcanic ash

Abstract

The eruption of Mount Semeru at the end of 2021 was responsible for emitting volcanic ash with specific characteristics. These unique mineralogy and chemical properties have both positive and negative effects on soil fertility, as excessive heavy metals adversely affect soil, plants, and the environment. Therefore, this study aimed to determine the distribution of volcanic ash cover from the eruption of Mount Semeru and investigate elemental composition as well as mineral characteristics of volcanic ash and soil covered by volcanic ash. The investigation was carried out in Supiturang village, Pronojiwo District, Lumajang, East Java, Indonesia. Sampling was carried out following the toposequence method, covering agricultural land within approximately ± 15 km from Mount Semeru. Pure volcanic ash was collected at sites not contaminated with soil. At the site location, it was found that the depth of volcanic ash cover ranged from "thin" (<2 cm) to "very thick" (>10 cm). The results of SEM and XRD analyses showed that of the pure volcanic ash contained quartz (50%), rock fragments (15%), plagioclase (12%), hornblende (10%), opaque (8%), and pyroxene (5%) minerals. The results of XRF analysis showed that the dominant elements in volcanic ash and soil were silica (Si), aluminum (Al), calcium (Ca), iron (Fe), and potassium (K). Several non-essential heavy metal elements found were Pb, Sn, and As, while rare minerals discovered were Y, Nb, Eu, and Yb at relatively low concentrations. The SEM analysis showed the structure of volcanic ash dominated by prismatic and blocky.

To cite this article: Setiawati, T.C., Nurcholis, M., Basuki, Budiman, S.A. and Yudiantoro, D.F. 2024. Elemental composition and mineralogical characteristics of volcanic ash and soil affected by the eruption of Mount Semeru, East Java. Journal of Degraded and Mining Lands Management 11(3):0000-0000, doi:10.15243/jdmlm.2024.113.0000.

Introduction

Mount Semeru is an Indonesian volcano that experiences multiple eruptions, similar to other regions such as Merapi, Sinabung, Kelud, and Agung. The eruption of Mount Semeru in December 2021 was significantly large, with lasting effects on the surrounding population, the environment, and the land. Volcanic eruptions emit material such as lava, sand, dust, and ash, accumulating on the peaks, slopes, foothills, and the surrounding area. The eruption from December 2021 to early 2022 resulted in a thick layer of volcanic ash covering several affected locations, including the Curah Kobokan, Supiturang village, and others. The ground surface in areas of volcanic eruption is generally covered by pyroclastic flows, Tephra (volcanic ash), and lava (Saputra et al., 2022). The eruption is considered detrimental, leading to the death of the surrounding vegetation and damage to agricultural land. Volcanic ash potentially causes severe disturbances in the infrastructure and human health (Barsotti et al., 2010), physically affecting the clogging intake structures, increasing turbidity, acidification, fluoride contamination, and other contaminants. The major leachate components are sulfate, Cl, Na, Ca, Mg, F, and minor leachate including Mn, Zn, Ba, Se, Br, B, Al, Si, Cd, Pb, As, Cu, Fe (Stewart et al., 2006). Furthermore, these negative impacts depend on several parameters, namely thickness, duration, and level of ash fall, as well as the grain size, chemical compounds, surface chemistry, and moisture content (Jones and BéruBé, 2011).

Volcanic materials play a crucial role in the rejuvenation process, positively affecting the agricultural aspects by enhancing soil fertility over time. These materials ejected from volcanoes rejuvenate soil and provide nutrient reserves, improving soil quality and crop yields (Minami et al., 2016). Some studies have investigated the effects of volcanic eruptions on soil microorganisms. The microbial activity is stimulated after volcanic eruptions, and the microbes have a substantial capacity to respond to volcanic disturbances (Berenstecher et al., 2017). With the thickness of the volcanic deposit, the phosphate-solubilizing bacteria (PSB) population and organic C dropped. Organic C levels were lower in the impacted than in the unaffected areas; low levels were detected at >20 cm, which can be attributed to organic materials that had accumulated in the topsoil prior to the volcanic eruption and were subsequently covered by volcanic deposits. Organic carbon thickness and distance from the crater had a significant impact on its ability to decrease the PSB population. The population of bacteria varied between 10^3 and 10^4 CFU g^{-1}. P solubilization activity was shown by the isolated bacteria (Ustiatik et al., 2023). Apart from affecting soil microorganisms, volcanic ash affects the physical and chemical properties of soil. Simanjuntak et al. (2015) reported that two years after the eruption of Mount Sinabung, there was a significant increase in cation exchange capacity (24.88 cmol kg^{-1}), total N (0.20%), and Ca (3.81 cmol kg^{-1}). Meanwhile, Fiantis et al. (2010) recorded a cation exchange capacity of 21.34 cmol kg^{-1}, while unaffected soil was around 17.27 cmol kg^{-1}, four years after the eruption. (Lubis et al., 2021) stated that 10 years after the eruption of Mount Sinabung in Sumatra, there was an increase in pH (H_2O), base cations, cation exchange capacity, and soil organic C. Several studies have indicated that volcanic eruptions disperse volcanic ash, covering areas up to several kilometers from the center of the eruption (Nurfiani and Bouvet de Maisonneuve, 2018; Cahyadi et al., 2024). Generally, volcanic ash consists of material originating from volcanism in the form of eruption comprising rock fragments, minerals, and volcanic glass, with particles measuring less than 2 mm (0.079 inch) in diameter. The term volcanic ash is often used to refer to all explosive fallout products (Tephra), including particles larger than 2 mm.

Characteristics of volcanic ash are influenced by minerals originating from magma, which show several dominant elements, including SiO_2, Al_2O_3, CaO, Fe_2O_3, MgO, K_2O, and Na_2O (Siddique, 2011). The mineralogical composition of these minerals depends on eruption conditions and magma configuration, which are often present in varying proportions, with additional oxides occasionally found in lower quantities. Wasis et al. (2017) stated that the chemical content in weight % of Mount Semeru eruption dust particles taken at a distance of 10 km from the peak is dominated by non-gas elements. These include carbon (40.393%), silicon (7.044%), aluminum (3.578%), calcium (2.237%), iron (3.047%), and magnesium (0.338%), while the main gas elements that make up the sampled dust particles is oxygen (41.865%). Latif et al. (2016) reported that the use of SEM-EDS test obtained Si content of the three types at Merapi, Sinabung, and Kelud, ranging from 45-60%, while elements of Al range 14-20%. Furthermore, various XRF results from volcanic ash from several volcanic eruptions in Indonesia are presented in Table 1.

Table 1. Oxide composition of the different volcanic ashes from the previous study.

Eruption	Elements (Oxides)									References
	SiO_2	Al_2O_3	CaO	MgO	Fe_2O_3	Na_2O	K_2O	TiO_2	MnO	
Talang	57.61	16.16	4.79	1.88	5.39	2.51	1.84	0.67	0.08	Fiantis et al. (2010)
Merapi	52.53	18.69	8.96	2.89	9.17	3.71	2.10	1.45	0.22	Wahyuni et al. (2012); Anda and
	56.39	19.34	7.32	1.44	7.15	3.92	2.10	0.65	0.16	Suparto (2016)
Sinabung	58.10	18.30	2.92	2.95	7.09 (FeO)	1.70	0.12	0.71	0.16	Fiantis et al. (2010)

Land management after the eruption of Mount Kelud volcano in 2014, with different cultivation patterns, has been researched by Saputra et al. (2022), showing Post-eruption volcanic ash thickness varied between land-use systems and was influenced by the plot's slope position rather than canopy cover. The average soil texture and porosity did not vary significantly between the periods. Initially, surface volcanic ash and soil layers had low aggregate stability and limited soil infiltration, demonstrating hydrophobicity. While organic C slowly increased from low levels in the fresh volcanic ash, the surface litter layer, aggregate stability, and soil infiltration quickly recovered. Different land use management resulted in different recovery trajectories of soil physical properties and function over the medium to long term after volcanic ash deposition.

The presence of volcanic ash with negative and positive effects from volcanic eruption needs to be investigated for environmental management, particularly soil. Therefore, this study aimed to determine the distribution of volcanic ash cover from the eruption of Mount Semeru and characterize its elemental and mineralogical compositions.

Materials and Methods

Preparation of maps

The preparation of a map illustrating the distribution of volcanic ash cover was carried out in several stages.

Field survey and data collection

The survey was carried out following the procedures from previous studies to delimit the study area and determine observation points as well as sample collection. Surveys and sampling were based on (1) the presence of pure volcanic ash, (2) soil covered by volcanic ash, and (3) soil not covered by volcanic ash. Subsequently, the locations of affected areas were determined administratively, with Supiturang Village consisting of 31 locations and an additional 5 points I in Sumberwuluh Village, as shown in Figure 1. The two villages are in the Pronojiwo District, Lumajang Regency, astronomically located between 112.92-113.01 East Longitude and 8.11-8.20 South Latitude.

Determining points for observing the depth of volcanic ash

The determination process was carried out using the grid sampling method on a representative basis with the Global Positioning System (GPS) tool to determine coordinate points. The number of points to be taken was adjusted to the survey level, characterized by moderate intensity with an output map scale of 1:75,000. The density of observations was set at one sample representing 25-50 ha (Wahyunto et al., 2016).

Interpolation

In preparing maps of areas affected by volcanic ash, interpolation was carried out to estimate aerial points not represented by sample points. In this study, interpolation used the menu provided by ArcToolbox in ArcGIS software, which can create a distribution from the results of several observation data points. The interpolation method used was the Inverse Distance Weighted (IDW) method, where two parameters were varied with an optionally variable search radius. This adaptability ensures that the radius changes according to the sample distribution, effectively covering the number of samples used for interpolation. Analysis of the thickness distribution of volcanic ash and other materials was carried out after the eruption in 2022.

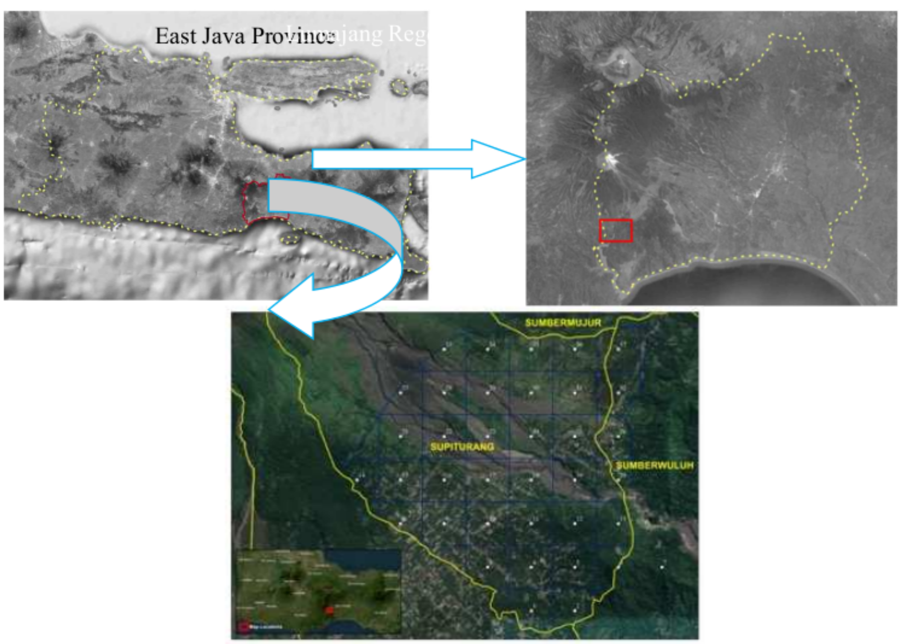

Figure 1. Research location and point for observation of the volcanic ash depth.

Sampling and characterization analysis of volcanic ash and soil mineralogical and chemical properties

The sampling of volcanic ash and soil was carried out on agricultural land, with the furthest distance being ± 9-15 km from the peak of Mount Semeru. Pure volcanic ash was collected at a location that was not contaminated with soil. On agricultural land, soil samples were taken at a depth of 0-20 and 20-40 cm with sugar cane vegetation cover for unaffected soil (12-21 cm). The specific coordinates were S 08º 10' 11.60" and E 113º 00' 19.66", taken approximately ± 9-12 km from the peak of Mount Semeru. Meanwhile, uncovered soil was taken at a location 15-16 km away with coordinates S 08º 09' 15.80" and E 113º 01' 26.97", with fairly dense pine vegetation and headers covering each other. Pure volcanic ash was collected from ash stuck to walls covered with roof tiles, ensuring it remained uncontaminated with soil or water at a distance of ± 9-12 km from the peak of Mount Semeru. Subsequently, volcanic ash sample preparation for analysis was ground to a size of ± 140 mesh.

Analysis of volcanic ash and soil

Mineral composition analysis of bulk samples and the clay fraction was carried out using the Smartlab version of X-ray diffraction (XRD) at the UPNVY Petroleum Engineering Laboratory, with the interpretation of mineral types based on the Handbook of Mineralogy (Anthony et al., 2001). The clay fraction was separated by making a suspension of the sample, and NaOH was added to increase the pH of the suspension to 10. This was followed by pipetting, which was carried out after leaving it for 3 hours and 30 minutes using the principle of Stokes' law. The sample collected was washed to remove ash covering the mineral crystals and filtered with cloth. Material that did not pass through the filter was identified using a polarizing microscope and connected to a computer to observe the mineral properties and grain size. The UPNVY Geological Engineering Laboratory microscopically analyzed mineral types using a Meiji Techno brand polarization microscope.

Mineral types were determined based on color, crystal shape, degree of roundness, and size. Elements content/composition analysis using X-ray fluorescence (XRF) Epsilon 4 brand EDXRF Unit with Rh-tube was carried out at the Yogyakarta Radiation Laboratory (Chemical Testing Sub-Laboratory). Topographic and morphological analysis tests as well as element identification in volcanic ash and soil using the pointing or mapping method. This analysis was facilitated using FESEM Thermo Scientific Quattro S completed with EDS Detector, WetSTEM, Heating, and Tensile Stage, which were carried out at the Cibinong Advanced Characterization Laboratory (ILAB) Cibinong Bogor. The particle size distribution of fresh volcanic ash was determined using the pipette method. Silt and clay fractions were measured after sedimentation according to Stokes' law. Subsequently, the sand fraction was separated into fine (50-200 m), medium (200-500 m), and coarse (500-2,000 m) using the wet sieving method. Calculation of chemical index weathering included "Product of Weathering Index" and "base loss values," each of which was calculated based on the equation:

Product of Weathering Index [PWI] = $[SiO_2/(TiO_2 + Fe_2O_3 + SiO_2 + Al_2O_3)] \times 100$

Base loss value = $[Al_2O_3/(CaO + MgO + K_2O)] \times 100$

Results and Discussion

Map of distribution of volcanic ash cover

The volcanic activity of Mount Semeru occurred in Lumajang Regency, East Java, between December 2021 and January 2022. During this period, the volcano produced volcanic ash, which was formed when gases dissolved in magma expanded and escaped suddenly into the atmosphere. Other products included pyroclastic flows, large lahars, incandescent landslides, and eruptions, causing buried land and significant damage. The force of the gases destroyed the magma and pushed it into the atmosphere, resulting in the solidification of fragments of volcanic rock and volcanic glass.

A map illustrating the distribution of volcanic ash covering agricultural areas was generated through biophysical observations, showing the depth on the land surface, as presented in Figure 2. Following the conditions and initial survey, volcanic ash and soil sampling were carried out in the affected area. The cover ranged from 2 cm to 21 cm on some vegetation at a distance of 11-13 km from the center of the eruption. Based on the mapping results, land area data with a thickness of between 2 cm and 12 cm covered 32.23% of the area, while 12 cm-21 cm covered 25.82%, namely 356.80 ha. The total area of land mapped to determine the impact of volcanic ash on land cover was 1381.59 ha, influencing the physical, chemical, and biological properties of soil, as presented in Figure 3. According to Rudianto et al. (2017), the rate of soil infiltration decreased as thickness increased, where 8-14 cm resulted in a very slow rate at 0.45-0.57 mm $hour^{-1}$ while 4 cm at 2.94 mm $hour^{-1}$, and uncovered soil recorded 4.89 mm $hour^{-1}$.

Elements composition of volcanic ash and soil

The major components found in both volcanic ash and soil included silica (Si), aluminum (Al), and iron (Fe). Concentrations of K and Ca cations were higher in volcanic ash than in soil (Table 2). This phenomenon occurred because the addition of volcanic ash resolved the defect of K and Ca cations in the soil. Meanwhile, Mg, Fe, and Mn concentrations were high in soil, as most of the elements in volcanic ash show corresponding amounts to those originating in soil.

Based on its silica content, sandstone resulting from volcanic eruption was grouped into acid volcanic rock (SiO_2 content >65%), medium (35-65%), and alkaline (<35%) (Lee et al., 2012). According to Le Maitre et al. (2002), the silica content can be divided into five groups, namely rhyolite (100-70%), dacite (70-62%), andesite (62-58%), basaltic andesitic (58-53.5%), and basalt (53.5-45%).

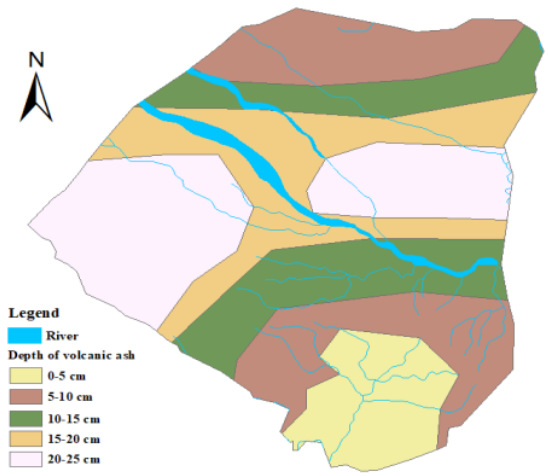

Figure 2. Map of the depth distribution of volcanic ash cover on the slopes of Mount Semeru.

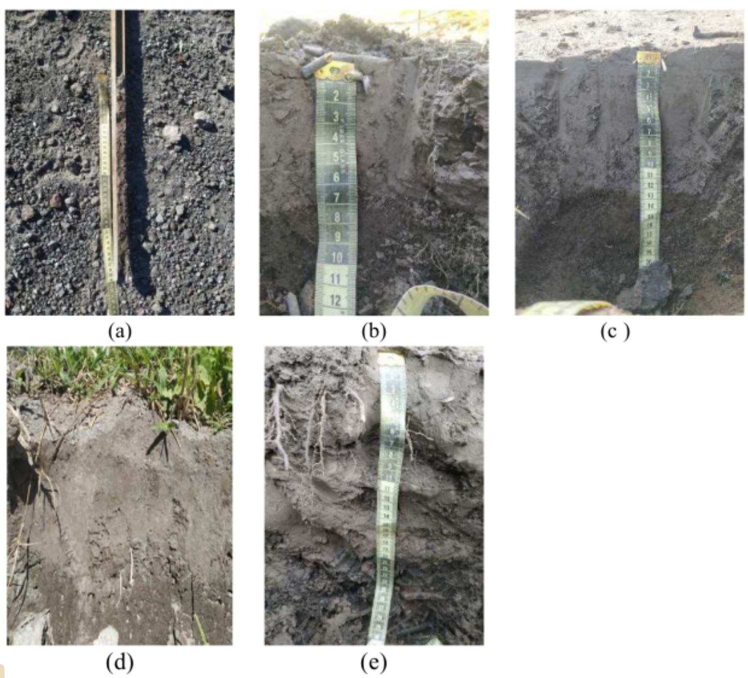

Figure 3. The thickness of volcanic ash in the field at a radius of 9-15 km: (a) thickness 0-5 cm, (b) thickness 5-10 cm, (c) thickness 10-15 cm, (d) thickness 15-20 cm, and (e) thickness 20-25 cm from the ground surface.

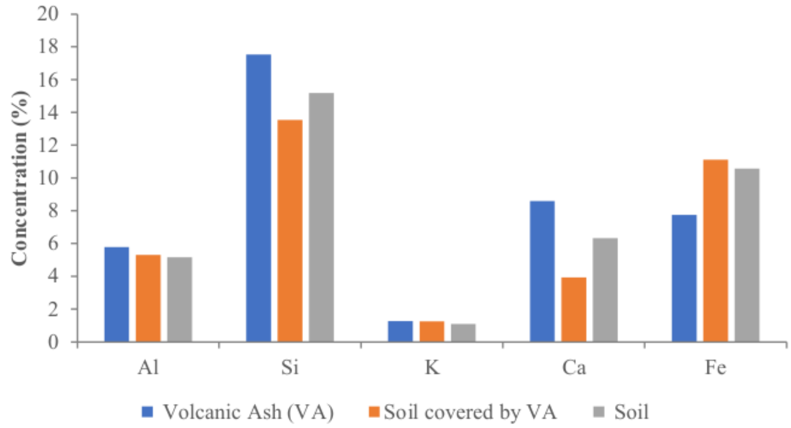

Figure 4. The five dominant elemental compositions of volcanic ash and soil.

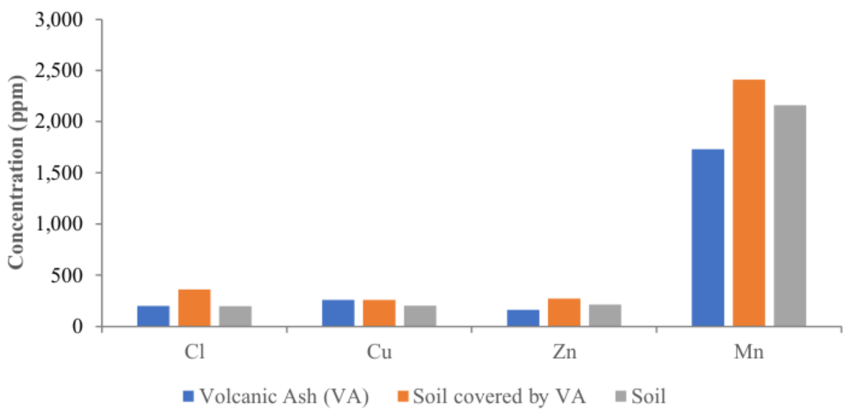

Figure 5. The concentration of micro-nutrients in volcanic ash and soil.

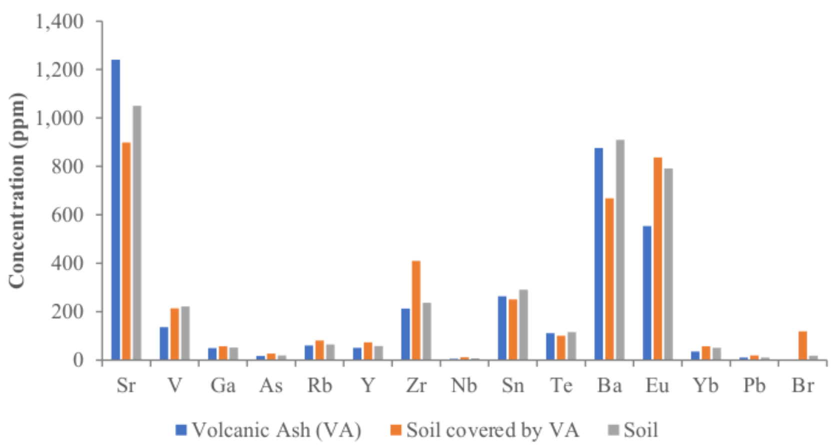

Figure 6. The concentration of non-essential elements and rare elements in volcanic ash and soil.

Table 2. Elemental compositions of volcanic ash and soil (XRF analysis).

Element	Concentration (%)		
	Volcanic Ash (VA)	Soil covered by VA	Soil
Si	17.52	13.54	15.18
Al	5.79	5.31	5.16
Fe	7.75	11.12	10.56
Ca	8.60	3.93	6.33
K	1.27	1.25	1.09
Mn	0.173	0.241	0.216
Mg	0.113	0.114	0.114

XRF analysis of volcanic ash showed that the concentration of silicate was the most considerable element, ranging from 18.00% to 37.48% in the form of silicate oxide (SiO_2). According to the SiO_2 content, volcanic ash obtained from the eruption of Mount Semeru 2021 is classified as "moderate volcanic" (Lee et al., 2012) and "basalt" (Le Maitre et al., 2002), as supported by the discovery of extrusive basalt and andesite igneous rocks on the slopes (Figure 7). Apart from Si, elements Ca, Fe, and Al were also found in relatively high concentrations of 8.60%, 7.75%, and 5.79%, respectively. The exact composition was obtained from the eruption of Mount Bromo and Raung in 2015, indicating that Fe, Si, Ca, and Al were the dominant elements. Quantitatively, Fe was the most dominant in these two volcanoes, namely 35.40% (Mount Bromo) and 43.00% (Mount Raung). The other elements found were Ba, Cr, Cu, Mn, P, Ni, Zn, Sb, Sr, and V with minor concentrations (Wardoyo et al., 2020). Apart from the essential nutrient elements such as K, Mg, Cu, Mn, Zn, Fe, S, and Cl, several heavy metals were also found in Mount Semeru, including Pb, Rb, and Ba, as well as rare elements, namely Nb, Y, Eu, etc. (Figure 6).

Figure 7. Rocks on the slopes of Mount Semeru after the eruption.

High levels of Si, Al, and Fe in volcanic material have a very detrimental impact on plant growth and plant health. According to previous investigations, volcanic material cannot contribute nutrients to plants because it has not passed through complete weathering. Based on Chemical Weathering Index calculations, the Product of Weathering Index (PWI) value of volcanic ash is relatively high, namely 62.09. This value indicates that weathering has just occurred, while for land covered or uncovered by volcanic ash, the PWI value is 51.53 and 55.58, respectively. The PWI value indicates the movement of less mobile elements such as Si, Al, Fe, and Ti in the weathering of ash deposits. Moreover, a higher PWI value corresponds to fresher weathering, and a lower value indicates a longer weathering process. The loss of the base nutrients K, Ca, and Mg, which are mobile to Al (base loss) in volcanic ash (0.799), is lower than in soil, namely 1.391. This indicates the presence of unreleased K, Ca, and Mg elements within the volcanic ash.

Minegraphic description of volcanic ash

The mineragraphic analysis indicated that the fine loose sand samples were characterized by brownish grains, measuring 0.1-0.6 mm, with the composition of 40% heavy minerals and 60% fine volcanic ash of <0.1 mm. This fine sand showed that the grains or fragments were subrounded-angular in shape. Furthermore, the samples were composed of quartz minerals, rock fragments, plagioclase, hornblende, opaque minerals (hematite, magnetite), and pyroxene, as illustrated in Table 4 and Figure 8. Generally, volcanic ash is formed when gases dissolved in magma escape into the atmosphere and experience sudden expansion and release, with sizes <0.1 mm becoming dominant (60%). Those measuring between 0.1-0.6 mm constituted fine sand grains with a content of 40%. The influence of this gas can cause changes in the magma and explosion into the atmosphere, thereby leading to solidification into volcanic rock fragments and volcanic glass.

Minerals covered and mixed with soil over six months showed changes in composition, as illustrated in Table 3. In uncovered soil, the percentage of rock fragments was the highest compared to other minerals, comprising up to 40% and 10% in volcanic ash. These fragments have characteristics of black color, sub-rounded-angular shape, and measure 0.1-0.6 mm.

Table 3. Mineral composition of Mount Semeru volcanic ash, soil covered by volcanic ash, and soil.

Mineral	Characteristics	Amount (%)*		
		VA	Soil covered by VA	Soil
Quartz	milky white, sub-rounded-angular in shape, 0.1-0.6 mm in size, and up to a few <0.1 mm (F3)	15	15	15
Rock fragments	black, sub-rounded-angular in shape and measuring 0.1-0.6 mm (H8)	10	12	40
Plagioclase	translucent white, short prismatic, tabular, sub-rounded-angular, and measuring 0.1-0.6 mm (D8).	8	10	10
Hornblende	black, long prismatic shape, sub-rounded-angular, and measuring 0.1-0.6 mm (D1).	3	3	0
Mineral opaque	black, metallic luster (magnetite), and some reddish/oxidized (hematite), sub rounded-angular in shape and measuring 0.1-0.6 mm (A4).	2	2	8
Pyroxene	Green, short prismatic, tabular, sub-rounded-angular, and measuring 0.1-0.6 mm (E5).	2	3	2
Volcanic fine material	fine volcanic ash measuring <0.1 mm	60	55	25
	Total	100	100	100

* VA = volcanic ash.

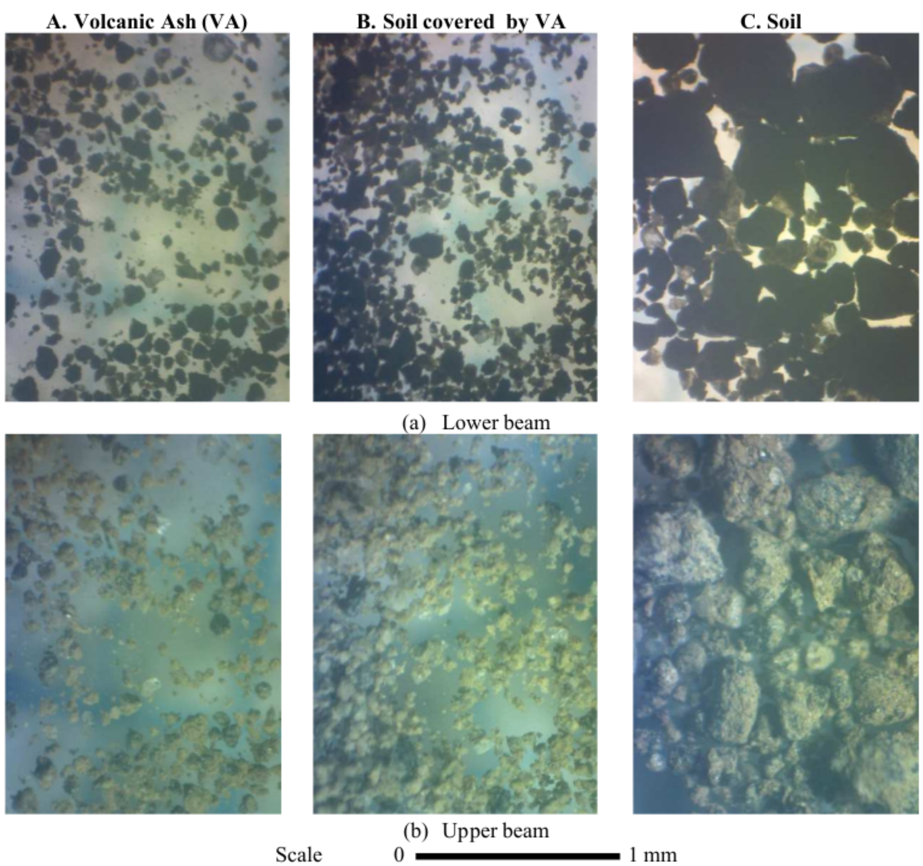

Figure 8. Results of mineral analysis using a polarizing microscope on volcanic ash, soil covered by volcanic ash, and soil.

Meanwhile, only 25% of the fine volcanic material measuring <0.1 mm in soil is not covered due to weathering processes, erosion, leaching, and infiltration due to rainfall. Hornblende is a member of the amphibole mineral group that weathers relatively quickly in the Bowen series. As presented in Table 3, hornblende was not found in soil (0%), but 3% was still identified in volcanic ash and soil covered by ash. The results of sand fraction distribution analysis (Figure 9) showed that volcanic ash was dominated by the "fine fraction" (0.25-0.10 mm) at 56.01% and the "very fine fraction" (0.10-0.05 mm) at 31.74%. Similarly, in covered or uncovered soil, the fine sand fraction was also dominant, but the percentage was less than 40%, indicating a higher distribution. This phenomenon occurred due to environmental conditions after the eruption, as rainfall carried the fine fractions in the soil to the location and the layers below, resulting in a reduced percentage of "fine" and "very fine" fractions. The results of the sand fraction distribution analysis were consistent with the outcomes of the microscopic mineral analysis, as presented in Table 3.

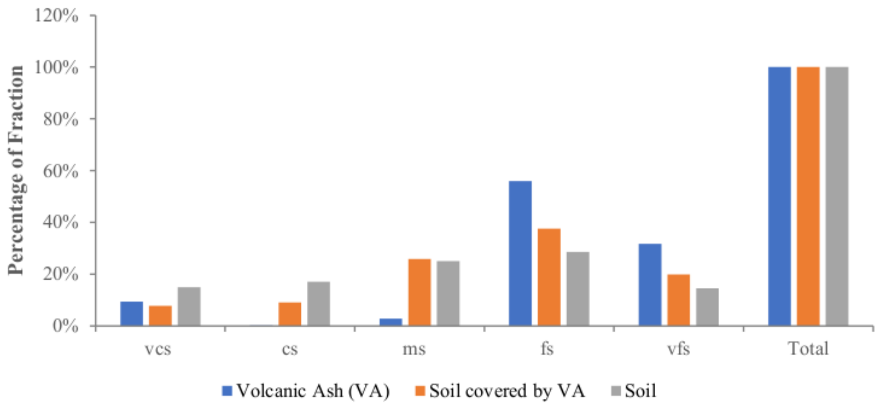

Figure 9. Sand fraction distribution analysis.

SEM-analysis

SEM (scanning electron microscopy) is a method used to determine the structure and surface morphology of thin-layer volcanic ash materials. This method enables the visualization of the surface morphology of crystalline structures. The results of observations conducted using SEM with 1,000x magnification showed that the structure of the erupted volcanic ash was in the form of prismatic and angular blocks (Figure 10a) of various sizes with a dominant size of 40µm-44µm, similar to the microscopic analysis (Table 3 and Figure 8A). In terms of texture, it showed few cavities or vesicles, indicating a relatively small amount of gas was trapped in ash during the crystallization process (Figure 10b). The texture of Mount Semeru volcanic ash differs from the eruption of the Merapi volcano in 2010, as well as Sinabung and Kelud volcanoes in 2014 (Latif et al., 2016). The SEM results on the three regions showed several hollow textures, indicating the presence of gas trapped during the magma-freezing process. In this study, volcanic material showed a sponge structure attached to the surface of the block with rounded to elongated shapes of various sizes (Figure 10c), as identified by (Latif et al., 2016). Figure 10d shows the results of Energy Dispersion Spectroscopy (EDS) at specific points on the sample from SEM analysis. In this analysis, X-rays are also emitted from the surface of the sample, carrying specific energy signatures for each element found in the sample. Subsequently, X-rays with various wavelengths are read by the EDS detector. Elements detected with the composition of the most significant percentages include O 45.5%, Si 32%, Al 8.2%, C 3.4%, Fe 3.1%, K 2.9%, Na 2.6%, Ca 2.1%, and Mg 0.3%. The composition of these elements shows a pattern as an oxide, with oxygen accounting for 45.5%, which is equivalent to the presence and percentage of elements Si, Al, and Fe. The difference between the analysis results using XRF (Table 2) and EDS (Figure 10) is caused by variation in the samples read. XRF analysis determines elemental composition and percentage in the bulk sample, while EDS focuses on specific spot samples. However, based on the results, both analyses provide similar percentage distribution patterns.

XRD analysis

The results of mineral analysis of bulk samples using XRD for Mount Semeru volcanic ash showed that the most dominant composition was Ca-feldspar (3.23Å) 42.05%, cristobalite (4.04Å) 10.82%, magnetite (2.51Å) 10.68%, hornblende (3.13Å) 10.63%, pyroxene (2.88Å) 10.40%, epidote (2.95Å) 7.60%, quartz (3.36Å) 4.86%, and pyrite was also found (1.61Å) 2.96%. Ca-feldspar was identified as the most dominant mineral through XRD analysis, accounting for 42.05%. Based on the results of element content analysis using XRF, the Ca content was 8.6%.

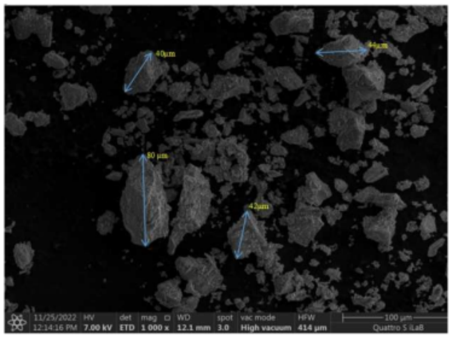

a

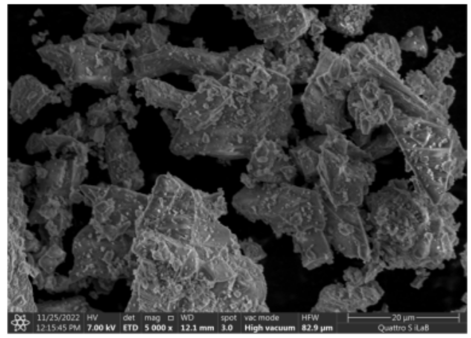

b

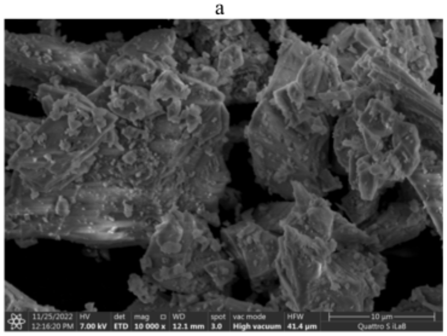

c

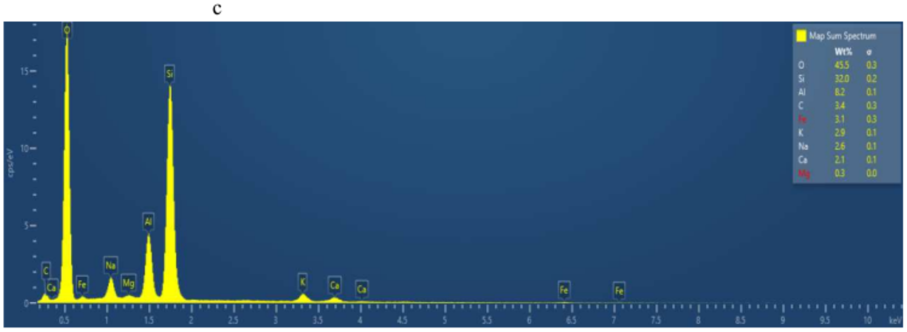

d

Figure 10. Volcanic ash graph.

The feldspar mineral identified using XRD with a peak of 3.23Å and a microscope was plagioclase, specifically Ca-feldspar ($CaAl_2Si_2O_8$). This mineral can be classified as anorthite ($CaAl_2Si_2O_8$), which is a type of plagioclase feldspar. The anorthite ($CaAl_2Si_2O_8$), together with albite ($NaAlSi_3O_8$), and K-feldspar (microcline, sanidine, orthoclase; $KAlSi_3O_8$) as the main feldspar minerals are abundant in various geological environments. Feldspars constitute approximately 50-60% of the total volume of the Earth's crust (Pakhomova et al., 2020), predominantly dominant by plagioclase, as part of the anorthite-albite series. XRD reading results of quartz (SiO_2) at 3.36Å and cristobalite (SiO_2) at 4.04Å showed that quartz added with cristobalite was 14.18%. This was similar to the 15% obtained using a microscope, where material with a very fine size (0.1 mm) with a percentage of 60% was not detected.

XRD analysis showed the presence of SiO_2 silica minerals at peaks 4.04Å (cristobalite) and 3.36Å (quartz). Cristobalite was found at 10.82% and quartz at 4.86%. Generally, this mineral was found in small volcanic ash grains (<0.1 mm in diameter). However, these minerals were not detected using a microscope (Table 3). Cristobalite is the silica polymorph of prime concern as it may crystallize, postextrusion, in volcanic lava domes, filling cracks and vesicles, so that it becomes a major mineral phase (up to 12 wt.%). Horwell et al. (2010) found that the cristobalite content in volcanic ash at Chaitén volcano (Chile-Argentina) was, on average, 2% after the eruption and increased 3 months later after the dome was formed to 16%, and quartz was found of 0.6-2.3 w%. The combination analysis of XRD and XRF can provide matching mineral types and quantification, but a thorough identification process is required (Hupp and Donovan, 2018). However, this analysis is challenging for samples that occur in nature, such as volcanic ash in this study. The type of mineral identified is based on the peak pattern characterized by minerals found and published in the Handbook of Mineralogy (Anthony et al., 2001). In this study, the composition of magnetite ($Fe^{2+}Fe^{3+}2O_4$) found was approximately 10.68%, potentially serving as a source of mining material for the extraction of metallic minerals. Volcanic sand material on the Kulon Progo beach in Yogyakarta, originating from Merapi volcanic material, contains iron (Fe), titanium (Ti), vanadium (V), cerium (Ce), chrome (Cr), arsenic (As) (Nurcholis and Mulyanto, 2017). Semeru volcanic material can also flow to lower locations, becoming metal minerals and rare earth elements (REE) with various concentrations (Figure 11), including yttrium (Y), zirconium (Zr), niobium (Nb), europium (Eu), tellurium (Te) and ytterbium (Yb). Some elements found in volcanic ash and soil after the eruption of Mount Semeru have been identified as material from Mount Merapi (Nurcholis and Mulyanto, 2017). Heavy metal and rare earth elements in volcanic materials are bonds with metal oxides, often referred to as impurities. Moreover, the adsorption of oxyanion such as As, Sb, and Cr, including Pb, Cd, Cu, Ni, and Zn metal on iron minerals, can occur through various processes, namely co-precipitation, adsorption, or phase transformation (Jiang et al., 2020; Shi et al., 2021).

The results on the presence of various types of heavy metal and rare earth elements (REE) are presented in Figure 11.

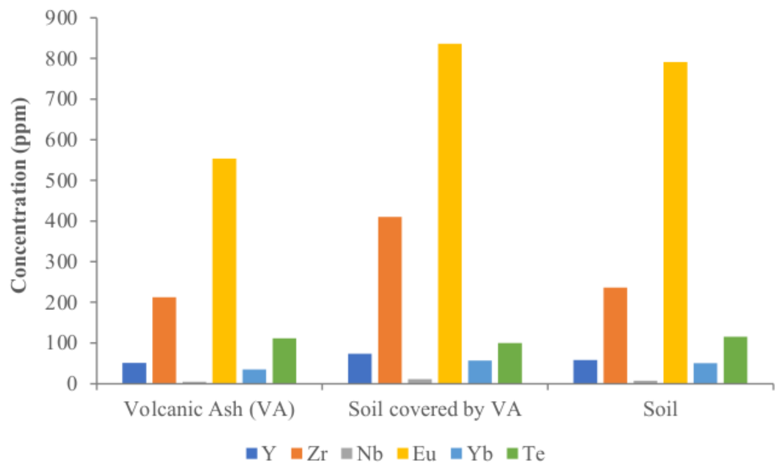

Figure 11. The concentration of rare earth elements (REE) in volcanic ash and soil.

XRD analysis identified pyroxene with a peak of 2.88Å (Figure 10), indicating a semi-quantitative concentration of 10.40%. Pyroxene mineral with the chemical formula (Ca, Na) (Mg, Fe, Al) $(Si, Al)_2O_6$ is a single-chain tetrahedral mineral group. In the formation and stability series compiled by brown, these minerals are classified as discontinuous series. Generally, pyroxene mineral is formed due to the magma crystallization process at high temperatures and is characterized by a single tetrahedral chain crystal structure, leading to high susceptibility to weathering. A negative charge is formed with isomorphic substitution, particularly for elements Si in tetrahedral formed by Al. This negative charge can be occupied by cations, which are quickly released into the solution phase during weathering. These elements become available for plant roots, making volcanic ash a valuable source of material that can be used as a mineral to provide nutrients. As a weatherable mineral, pyroxene serves as a rapid nutrient source in soil. The hornblende mineral with XRD readings at the peak of 3.13Å has a content of 10.63%. This mineral has a chemical formula $Ca_2(Mg, Fe, Al)_5(Al, Si)_8O_{22}(OH)_2$ and is included in the amphibole group mineral with a double chain tetrahedral arrangement. Although hornblende can also provide nutrients, it has higher stability and slower weathering rates due to the double-chain tetrahedral form. These differences in properties show that minerals in volcanic ash can act as reserves of elements available for a relatively long time. Furthermore, quartz SiO_2 mineral with a peak of 3.36Å and epidote mineral $Ca_2(Fe^{3+}, Al)_3(SiO_4)_3(OH)$ at 2.95Å were identified as minor minerals in volcanic ash material, consisting of semi-quantitatively percentages of 4.86% and 2.95%, respectively. The mineral pyrite (FeS_2) was found in volcanic ash studied with a peak of 1.61Å of 2.91%, as presented in Figure 12. As an iron sulfide mineral, pyrite can form in an environment characterized by a reduction reaction and is commonly found in materials such as volcanic ash. Moreover, volcanic ash from the eruption of Japan's Ontake volcano in 2014 showed the presence of pyrite minerals in relatively large quantities in coarse and medium-sized volcanic ash (Minami et al., 2016). Mineralogical analysis using a microscope can identify various minerals such as quartz, rock fragments, plagioclase, hornblende, opaque minerals, pyroxene, and volcanic fine material.

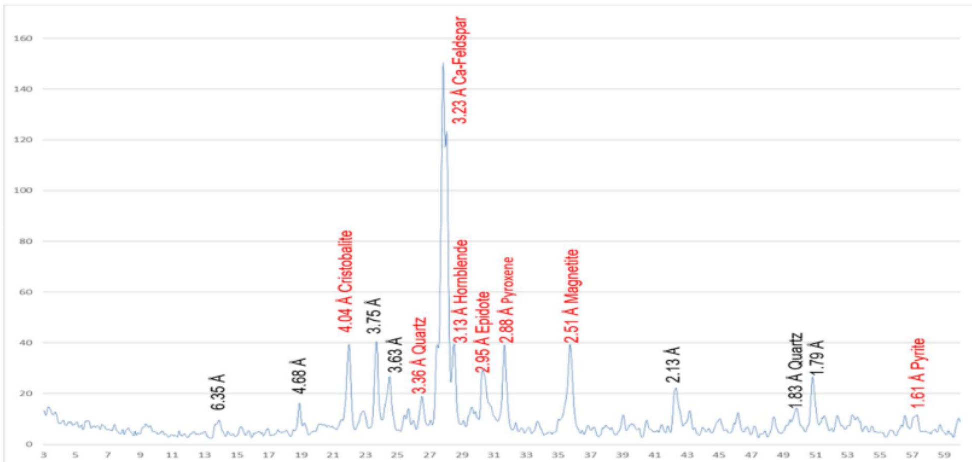

Figure 12. X-ray diffraction pattern of volcanic ash samples from Mount Semeru.
Note: red font indicates the main peak as a determinant of the type of mineral identified.

Based on the results of microscopic analysis, the minerals identified were pyroxene, plagioclase, and hornblende. XRD analysis also showed pyroxene, hornblende, and feldspar (plagioclase feldspar). According to the Bowen reaction series, the mineral composition was "intermediate", and the rock type was "diorite."

Conclusion

In conclusion, this study showed that the distribution of volcanic ash cover ranged from “thin” (<2 cm) to “very thick” (>12 cm), comprising 32.23% of the area, while 12 cm-21 cm covered 25.82%. The microscopic and XRD analysis of pure volcanic ash contained quartz minerals (50%), rock fragments (15%), plagioclase (12%), hornblende (10%), opaque minerals (8%), and pyroxene (5%). Elemental composition properties of volcanic ash and soil based on XRF analysis obtained several dominating elements, namely silica (Si), aluminum (Al), calcium (Ca), iron (Fe), and potassium (K). Non-essential heavy metal elements that were found included Pb, Sn, and As, while rare minerals were Y, Nb, Eu, and Yb, with low concentrations.

Acknowledgments

The authors are grateful to the entire team and students who have contributed to this study and appreciate the University of Jember for providing financial support through the PGB scheme. Furthermore, the authors are grateful for the facilities, scientific, and technical support received from Advanced Characterization Laboratories Cibinong-Integrated Laboratory of Bioproduct, and Radiation Laboratory Yogyakarta, National Research and Innovation Agency, and the Geological Engineering Laboratory, Faculty of Mineral Technology, Universitas Pembangunan Nasional Veteran Yogyakarta, for assistance provided during XRD and microscopic mineral analysis.

References

Anda, M. and Suparto, S. 2016. Characteristics of pristine volcanic materials: Beneficial and harmful effects and their management for restoration of agroecosystem. *Science of The Total Environment* 543:480-492, doi:10.1016/j.scitotenv.2015.10.157.

Anthony, J.W., Bideaux, R.A., Bladh, K.W. and Nichols, M.C. 2001. Handbook of mineralogy, Mineralogical Society of America. In Chantilly, VA20151-1110. USA.

Barsotti, S., Andronico, D., Neri, A., Del Carlo, P., Baxter, P.J., Aspinall, W.P. and Hincks, T. 2010. Quantitative assessment of volcanic ash hazards for health and infrastructure at Mt. Etna (Italy) by numerical simulation. *Journal of Volcanology and Geothermal Research* 192(1-2):85-96, doi:10.1016/j.jvolgeores.2010.02.011.

Berenstecher, P., Gangi, D., González-Arzac, A., Martínez, M.L., Chaves, E.J., Mondino, E.A. and Austin, A.T. 2017. Litter microbial and soil faunal communities stimulated in the wake of a volcanic eruption in a semi-arid woodland in Patagonia, Argentina. *Functional Ecology* 31(1), doi:10.1111/1365-2435.12683.

Cahyadi, M.N., Bawasir, A., Arief, S., Widodo, A., Rusli, M., Kusumawardani, D., Rahmawati, Y., Martina, A., Maulida, P. and Lestiana, H. 2024. Analysis of the effect of the 2021 Semeru eruption on water vapor content and atmospheric particles using GNSS and remote sensing. *Geodesy and Geodynamics* 15(1), doi:10.1016/j.geog.2023.04.005.

Fiantis, D., Nelson, M., Shamshuddin, J., Goh, T.B. and Van Ranst, E. 2010. Determination of the geochemical weathering indices and trace elements content of new volcanic ash deposits from Mt. Talang (West Sumatra) Indonesia. *Eurasian soil Science* 43(13):1477-1485, doi:10.1134/S1064229310130077.

Horwell, C.J., Le Blond, J.S., Michnowicz, S.A.K. and Cressey, G. 2010. Cristobalite in a rhyolitic lava dome: Evolution of ash hazard. *Bulletin of Volcanology* 72(2):249-253, doi:10.1007/s00445-009-0327-1.

Hupp, B.N. and Donovan, J.J. 2018. Quantitative mineralogy for facies definition in the Marcellus Shale (Appalachian Basin, USA) using XRD-XRF integration. *Sedimentary Geology* 371:16-31, doi:10.1016/j.sedgeo.2018.04.007.

Jiang, S., Yan, X., Peacock, C.L., Zhang, S., Li, W., Zhang, J., Feng, X., Liu, F. and Yin, H. 2020. Adsorption of Cr(VI) on Al-substituted hematites and its reduction and retention in the presence of Fe^{2+} under conditions similar to subsurface soil environments. *Journal of Hazardous Materials* 390, doi:10.1016/j.jhazmat.2019.122014.

Jones, T. and BéruBé, K. 2011. The bioreactivity of the sub-10μm component of volcanic ash: Soufrière Hills volcano, Montserrat. *Journal of Hazardous Materials* 194:128-134, doi:10.1016/j.jhazmat.2011.07.092.

Latif, D.O., Rifa'i, A. and Suryolelono, K.B. 2016. Chemical characteristics of volcanic ash in Indonesia for soil stabilization: Morphology and mineral content. *International Journal of GEOMATE* 11(4):2606-2610, doi:10.21660/2016.26.151120.

Le Maitre, R.W., Streckeisen, A., Zanettin, B., Le Bas, M.J., Bonin, B. and Bateman, P. 2002. *Igneous Rocks. A Classification and Glossary of Terms.* Recommendations of the International Union of Geological Sciences Subcommission on the Systematics of Igneous Rocks. 2nd Edition, Cambridge University Press., doi:10.1017/cbo9780511535581.

Lee, S., Hahn, C., Rhee, M., Oh, J.E., Song, J., Chen, Y., Lu, G., Perdana, and Fallis, A.G. 2012. Physical Geology: Earth Revealed, 9th Edition. In Climate Change 2013 - The Physical Science Basis Vol. 53, Issue 9.

Lubis, R.L., Juniarti, Rajmi, S.L., Armer, A.N., Hidayat, F.R., Zulhakim, H., Yulanda, N., Syukri, I.F. and Fiantis, D. 2021. Chemical properties of volcanic soil after 10 years of the eruption of Mt. Sinabung (North Sumatera, Indonesia). *IOP Conference Series: Earth and Environmental Science* 757(1), doi:10.1088/1755-1315/757/1/012043.

Minami, Y., Imura, T., Hayashi, S. and Ohba, T. 2016. Mineralogical study on volcanic ash of the eruption on 27 September 2014, at Ontake volcano, central Japan: Correlation with porphyry copper. *Earth, Planets and Space* 68(1), doi:10.1186/s40623-016-0440-2.

Nurcholis, M. and Mulyanto, D. 2017. Study on the residue resulted from the metallic minerals separations to the coastal iron sand of Yogyakarta, Indonesia. *International Journal of Applied Engineering Research* 12(15):5218-5225.

Nurfiani, D. and Bouvet de Maisonneuve, C. 2018. Furthering the investigation of eruption styles through quantitative shape analyses of volcanic ash particles. *Journal of Volcanology and Geothermal Research* 354:102-114, doi:10.1016/j.jvolgeores.2017.12.001.

Pakhomova, A., Simonova, D., Koemets, I., Koemets, E., Aprilis, G., Bykov, M., Gorelova, L., Fedotenko, T., Prakapenka, V. and Dubrovinsky, L. 2020. Polymorphism of feldspars above 10 GPa. *Nature Communications* 11(1):1-8, doi:10.1038/s41467-020-16547-4.

Rudianto, G., Indradewa, D. and Utami, S.N.H. 2017. Influence of volcanic ash thickness above the surface soil fall at various growth phases on the growth and yield of corn (*Zea mays*). *Vegetalika* 6(3):1-11, doi:10.22146/veg.27959 (*in Indonesian*).

Saputra, D.D., Sari, R.R., Hairiah, K., Widianto, Suprayogo, D. and van Noordwijk, M. 2022. Recovery after volcanic ash deposition: vegetation effects on soil organic carbon, soil structure and infiltration rates. *Plant and Soil* 474(1-2):163-179, doi:10.1007/s11104-022-05322-7.

Shi, M., Min, X., Ke, Y., Lin, Z., Yang, Z., Wang, S., Peng, N., Yan, X., Luo, S., Wu, J. and Wei, Y. 2021. Recent progress in understanding the mechanism of heavy metals retention by iron (oxyhydr) oxides. *Science of The Total Environment* 752:141930, doi:10.1016/j.scitotenv.2020.141930.

Siddique, R. 2011. Effect of volcanic ash on the properties of cement paste and mortar. *Resources, Conservation and Recycling* 56(1), doi:10.1016/j.resconrec.2011.09.005.

Simanjuntak, C.M., Elfiati, D. and Delvian, D. 2015. Impact of Mount Sinabung eruption on soil chemical properties in Karo Regency. *Peronema Forestry Science Journal* 4(4):53-58 (*in Indonesian*).

Stewart, C., Johnston, D.M., Leonard, G.S., Horwell, C.J., Thordarson, T. and Cronin, S.J. 2006. Contamination of water supplies by volcanic ashfall: A literature review and simple impact modelling. *Journal of Volcanology and Geothermal Research* 158(3-4):296-306, doi:10.1016/j.jvolgeores.2006.07.002.

Ustiatik, R., Ariska, A.P., Hakim, Q.L., Wicaksono, K.S. and Utami, S.R. 2023. Volcanic deposits thickness and distance from Mt Semeru crater strongly affected phosphate solubilizing bacteria population and soil organic carbon. *Journal of Ecological Engineering* 24(10):360-368, doi:10.12911/22998993/170860.

Wahyuni, E.T., Triyono, S. and Suherman, S. 2012. Determination of chemical composition of volcanic ash from Merapi Mt. Eruption. *Jurnal Manusia dan Lingkungan* 19(2):150-159, doi:10.22146/JML.18531 (*in Indonesian*).

Wahyunto, Hikmatullah, Suryani, E., Tafakresnanto, C., Ritung, S., Mulyani, A., Sukarman, Nugroho, K., Sulaeman, Y., Apriyana, Y., Suciantini, S., Pramudia, A., Suparto, Subandiono, R.E., Sutriadi, T. and Nursyamsi, D. 2016. Technical Instructions: Soil Survey and Mapping of Semi Detail Level 1:50,000 Scale. Center for Agricultural Land Resources Research and Development (*in Indonesian*).

Wardoyo, A.Y.P., Noor, J.A.E., Elbers, G., Schmitz, S., Flaig, S.T. and Budianto, A. 2020. Characterizing volcanic ash elements from the 2015 eruptions of Bromo and Raung volcanoes, Indonesia. *Polish Journal of Environmental Studies* 29(2):1899-1907, doi:10.15244/pjoes/99101.

Wasis, Juwono, A.M. and Susilo, A. 2017. Study of physical and chemical characterization of Mount Semeru dust. *Proceedings of the XII National Seminar on Industrial and Information Technology Engineering* 2017 *High School Yogyakarta National Technology*, 223-228 (*in Indonesian*).

Elemental composition and mineralogical characteristics of volcanic ash and soil affected by the eruption of Mount Semeru, East Java

ORIGINALITY REPORT

13%	11%	13%	7%
SIMILARITY INDEX	INTERNET SOURCES	PUBLICATIONS	STUDENT PAPERS

PRIMARY SOURCES

1	repo-dosen.ulm.ac.id Internet Source	2%
2	link.springer.com Internet Source	1%
3	scholar.unair.ac.id Internet Source	1%
4	www.pjoes.com Internet Source	1%
5	worldwidescience.org Internet Source	1%
6	R L Lubis, Juniarti, S L Rajmi, A N Armer, F R Hidayat, H Zulhakim, N Yulanda, I F Syukri, D Fiantis. "Chemical Properties of Volcanic Soil After 10 Years of the Eruption of Mt. Sinabung (North Sumatera, Indonesia)", IOP Conference Series: Earth and Environmental Science, 2021 Publication	1%

7	Submitted to School of Business and Management ITB Student Paper	1%
8	Markus Anda, Muhrizal Sarwani. "Mineralogy, Chemical Composition, and Dissolution of Fresh Ash Eruption: New Potential Source of Nutrients", Soil Science Society of America Journal, 2012 Publication	1%
9	Jin Chen, Yuqing Guo, Fansheng Li, Yaxin Zheng, Daolong Xu, Haijing Liu, Xinyan Liu, Xinyu Wang, Yuying Bao. "Exploring the effects of volcanic eruption disturbances on the soil microbial communities in the montane meadow steppe", Environmental Pollution, 2020 Publication	<1%
10	iieta.org Internet Source	<1%
11	www.kseeg.org Internet Source	<1%
12	Claire J. Horwell. "Cristobalite in a rhyolitic lava dome: evolution of ash hazard", Bulletin of Volcanology, 12/02/2009 Publication	<1%
13	Irene Rizky Safina Daulay, Harits Atika Ariyanta, Azizatul Karimah, Fitria et al.	<1%

"Preparation of superhydrophobic biomedical pulp from rice straw coated with a stearic acid-cellulose composite", Bioresource Technology Reports, 2024
Publication

14	www.bolivianchemistryjournal.org Internet Source	<1%
15	Submitted to University of Hong Kong Student Paper	<1%
16	www.ncbi.nlm.nih.gov Internet Source	<1%
17	Thomas Wilson. "Vulnerability of farm water supply systems to volcanic ash fall", Environmental Earth Sciences, 12/05/2009 Publication	<1%
18	Joaquim Araújo Nóbrega, Clésia Cristina Nascentes, Geórgia Cristina Labuto Araújo, Ana Rita Araújo Nogueira et al. "High-Throughput Microwave-Assisted Digestion and Extraction Procedures for Agricultural Materials", Communications in Soil Science and Plant Analysis, 2007 Publication	<1%
19	academictree.org Internet Source	<1%
20	d197for5662m48.cloudfront.net Internet Source	<1%

21	en.wikipedia.org Internet Source	<1%
22	scholar.unand.ac.id Internet Source	<1%
23	Shoroog Alraddadi, Hasan Assaedi. "Characterization and Potential Applications of Different Powder Volcanic Ash", Journal of King Saud University - Science, 2020 Publication	<1%
24	www.ivhhn.org Internet Source	<1%
25	Retno Leodita Lubis, Juniarti Juniarti, Saftia Laila Rajmi, Aldi Nanda Armer et al. "Chapter 78 Geochemical Weathering Indices of Volcanic Soil After the Eruption from Mount Sinabung in 2020", Springer Science and Business Media LLC, 2022 Publication	<1%
26	S L Rajmi, G Gusnidar, R L Lubis, F I Ginting, F R Hidayat, H Zulhakim, A N Armer, N Yulanda, I F Syukri, D Fiantis. "Improving Volcanic Soil Chemistry After the Eruption of Mt. Sinabung, North Sumatera in 2020", IOP Conference Series: Earth and Environmental Science, 2021 Publication	<1%
27	www.plr.ugent.be Internet Source	<1%